Radical Cations of Branched Alkanes in Solutions: Time-Resolved Magnetic Field Effect and Quantum Chemical Studies

ARTICLE *in* THE JOURNAL OF PHYSICAL CHEMISTRY A · MARCH 2012

Impact Factor: 2.69 · DOI: 10.1021/jp2113208 · Source: PubMed

6 AUTHORS, INCLUDING:

Pavel Potashov
Russian Academy of Sciences
6 PUBLICATIONS **20** CITATIONS
SEE PROFILE

Vsevolod I Borovkov
Russian Academy of Sciences
61 PUBLICATIONS **353** CITATIONS
SEE PROFILE

Nina Gritsan
Russian Academy of Sciences
168 PUBLICATIONS **2,055** CITATIONS
SEE PROFILE

V. A. Bagryansky
Russian Academy of Sciences
51 PUBLICATIONS **391** CITATIONS
SEE PROFILE

THE JOURNAL OF PHYSICAL CHEMISTRY A

Article

pubs.acs.org/JPCA

Radical Cations of Branched Alkanes in Solutions: Time-Resolved Magnetic Field Effect and Quantum Chemical Studies

Pavel A. Potashov,*[,†] Vsevolod I. Borovkov,[†,‡] Lyudmila N. Shchegoleva,[§] Nina P. Gritsan,[†,‡] Victor A. Bagryansky,[†,‡] and Yuriy N. Molin[†]

[†]Institute of Chemical Kinetics and Combustion, Siberian Branch of the Russian Academy of Sciences, 3, Institutskaya street, Novosibirsk 630090, Russia

[‡]Novosibirsk State University, 2 Pirogova street, Novosibirsk 630090, Russia

[§]N.N. Vorozhtsov Novosibirsk Institute of Organic Chemistry, Siberian Branch of the Russian Academy of Sciences, 9 Lavrentiev avenue, Novosibirsk 630090, Russia

ABSTRACT: Radical cations of heptane and octane isomers, as well as several longer branched alkanes, were detected in irradiated *n*-hexane solutions at room temperature by the method of time-resolved magnetic field effect (TR MFE). To identify radical cations, the hyperfine coupling constants as determined by simulation of the TR MFE curves were compared to the constants calculated using the density functional theory (DFT) approach. The *g*-values of the observed radical cations were close to that of the 2,2,3,3-tetramethylbutane radical cation studied earlier by optically detected electron spin resonance (ESR) and TR MFE techniques. No evidence of the decay of the radical cations of branched alkanes to produce olefin radical cations was found, which was further supported by the observation of positive charge transfer from the observed radical cations to cycloalkane molecules. The lifetimes of the radical cations of the branched alkanes were found to be longer than tens of nanoseconds.

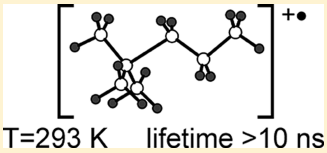

1. INTRODUCTION

The radical ions of organic compounds are very reactive intermediates participating in various chemical processes.[1] The importance of radical ions in chemistry and biology stimulates interest in their structure and reactivity. The radical ions of aromatic hydrocarbons have been successfully investigated in solutions by conventional ESR. However, the ESR spectra of the radical cations (RCs) of aliphatic hydrocarbons have been mainly recorded under their stabilization in irradiated low-temperature matrices.[2]

In solutions, the lifetimes of alkane RCs formed under ionizing radiation are rather short due to the high rate of geminate recombination and fast mono- and bimolecular reactions. In particular, the proton transfer from RCs to a solvent molecule and the elimination of a dihydrogen molecule from RCs have been discussed.[2,3] The pulse radiolysis experiments demonstrated that the lifetimes of RCs escaping geminate recombination are within hundreds of nanoseconds for RCs of cyclic alkanes,[4,5] while *n*-alkane RCs decay on a time scale from several to tens of nanoseconds.[6] The failure to detect neopentane and 2,2,4-trimethylpentane RCs by the pulse radiolysis technique[7] led to the conclusion that the lifetimes of branched alkane RCs in solutions fall into the subnanosecond time domain.[5,7]

The methods of spin chemistry, such as optically detected ESR,[8] time-resolved magnetic field effect (TR MFE),[9] and spectroscopy of magnetically affected reaction yield (MARY spectroscopy),[10] open new opportunities for the study of short-lived alkane RCs.

The optically detected ESR was used to observe RC of 2,2,3,3-tetramethylbutane in liquid alkanes.[3,11] Yet attempts to detect the other branched alkanes RCs in liquid solutions have failed.

The most promising approach is the application of TR MFE,[9] which combines the merits of ESR with the pulse radiolysis technique. In the method of TR MFE, the decay of recombination fluorescence modulated by singlet−triplet transitions in geminate pair is recorded. Experimental conditions are chosen in such a way that the pair of the recombining radical ions consists of the desired alkane RC and a radical anion of a fluorophore.

In addition to the RCs of *n*-alkanes,[12] we have recently succeeded in detecting several branched alkane RCs. The parameters of the ESR spectra of RCs of 2,2,3,3-tetramethylbutane,[11] 2,3-dimethylbutane, and 2,2,4-trimethylpentane[13] have been obtained. Their lifetimes in solutions at room temperature were found to be no less than 10 ns.

The present study was undertaken to extend the range of the branched alkanes RCs studied by TR MFE and to better understand their properties.

2. EXPERIMENTAL AND COMPUTATIONAL DETAILS

Materials and Methods. As in our earlier works,[11−13] the radical cations under study, $RH^{+\bullet}$, were generated in *n*-hexane solution using the X-ray pulses of about 2 ns duration. Created by direct ionization, the solvent radical cations transfer their positive charge to molecules of the added alkane to form $RH^{+\bullet}$. The RH concentration was chosen no less than 30 mM to

Received: November 24, 2011
Revised: February 24, 2012
Published: March 20, 2012

   dx.doi.org/10.1021/jp2113208 | *J. Phys. Chem. A* 2012, 116, 3110−3117

ensure fast (<1 ns) charge transfer. On the other hand, this concentration was typically less than 1 M to avoid any undesirable influence of the impurities in the branched alkane. As electron acceptor and fluorophore, *p*-terphenyl-d_{14} (*p*TP) was used at a concentration of about 30 μM, which is low enough to preclude the positive charge transfer to *p*TP within the time range of interest. In these conditions, the predominant contribution to the delayed fluorescence results from recombination of singlet correlated pairs $RH^{+\bullet}/pTP^{-\bullet}$ at times >1 ns.

In the experiments, the decays of the delayed fluorescence intensity of the irradiated solutions were recorded at 293 K in the single photon counting mode using a nanosecond X-ray fluorimeter, as described elsewhere.[14] To extract the temporal evolution of the singlet spin state population of the spin correlated pairs, the fluorescence decay curves from the same solution were recorded in a magnetic field of up to 1.1 T and in zero (<0.05 mT) field.

Particular attention was paid to the solvent purification from impurities of unsaturated hydrocarbons. The *n*-hexane was treated by sulfuric acid, washed repeatedly with water, dried, and distilled over Na. In addition, it was passed several times through a column with alumina. By means of gas chromatography, we found that in used *n*-hexane the main alkane impurities were 2-methylpentane (typically 0.2% v/v), 3-methylpentane (0.3%), and methylcyclopentane (0.1%).

Squalane (Aldrich, 99%), 2,6,10,14-tetramethylpentadecane (Sigma, 98%), and 2,2,4,4,6,8,8-heptamethylnonane (Aldrich, 98%) were passed through columns with Al_2O_3. 2,2,3-Trimethylbutane (Fluka, 99%), 2,2-dimethylpentane (Aldrich, 99%), 2,4-dimethylpentane (Aldrich, 99%), 3,3-dimethylpentane (Aldrich, 99%), 2,5-dimethylhexane (Aldrich, 99%), isopropylcyclohexane (Aldrich, 99%), *tert*-butylcyclohexane (Aldrich, 99%), 2-methylpentane (Aldrich, 99%), 3-methylpentane (Aldrich, 99%), 1,3-dimethyladamantane (Aldrich, 99%), *trans*-decalin (Aldrich, 99%), and *p*-terphenyl-d_{14} (Alldrich, 98%) were used as received.

Quantum Chemical Calculations. To support the assignment of the TR MFE to a specific alkane RC, the isotropic hyperfine coupling (HFC) constants of the assumed RCs were calculated at the UB3LYP/6-31G(d) level.[15] The structures of different conformers of RCs were optimized at the same level of theory. All calculations were performed using GAMESS[16] (2,2,3-trimethylbutane, 2,2-dimethylpentane, isopropylcyclohexane, *tert*-butylcyclohexane) or Gaussian 03[17] (2,4-dimethylpentane, 3,3-dimethylpentane, 2,5-dimethylpentane) suites of programs. We did not calculate the HFC constants for three bulky RCs (2,6,10,14-tetramethylpentadecane, 2,2,4,4,6,8,8-heptamethylnonane, and squalane).

In solution at ambient temperature, the alkane RCs exist in different conformations, which transform into each other by the internal rotation of fragments about C−C bonds. These transformations modulate the HFC constants. Thus, the existence of different conformations was taken into account to correctly compare the calculated and experimental HFC constants. For heptane and octane isomers, we calculated the HFC constants for all low-energy conformations and then averaged them over these conformations with the Boltzmann weighting factor. This was done in the framework of two simplifying assumptions:

(1) The internal rotation is so fast that the approximation of fast exchange limit between the radical ESR spectrum lines is valid.

(2) Calculations of HFC constants were carried out only for the conformations, corresponding to local minima at potential energy surface.

The conformations were obtained from the basic one by rotating the fragments about the C−C bonds by ±120° followed by subsequent geometry optimization. Note that rotating either methyl groups or a *tert*-butyl fragment by 120° restores the RC geometry, and therefore the optimization is not required.

TR MFE: Theoretical Background. The method of TR MFE is based on the effect of dynamic transitions between the singlet and triplet states of a spin-correlated radical ion pair on the yield of the singlet-excited (fluorescing) products of the pair recombination.

The TR MFE is defined as the ratio of recombination fluorescence kinetics measured with ($I_B(t)$) and without ($I_0(t)$) applied magnetic field. This ratio is expressed as follows:[9]

$$\frac{I_B(t)}{I_0(t)} = \frac{\theta\rho_{ss}^B(t) + \frac{1}{4}(1-\theta)}{\theta\rho_{ss}^0(t) + \frac{1}{4}(1-\theta)} \quad (1)$$

where θ is the fraction of pairs formed in the spin-correlated singlet state, $\rho_{ss}(t)$ is a function describing the evolution of the population of the singlet state of such pairs, and indices "B" and "0" denote the values in a high and zero magnetic field, respectively.

The evolution of pair spin population is described in terms of the same parameters (HFC constants, *g*-factor, and paramagnetic relaxation times) as the conventional ESR spectrum. These parameters can be derived either from simulation of the TR MFE curves or (for simple cases) directly from features of these curves. The $\rho_{ss}(t)$ functions in high and zero magnetic fields have the form:[9]

$$\rho_{ss}^B(t) = \frac{1}{4} + \frac{1}{4}e^{-t/T_1} + \frac{1}{2}e^{-t/T_2}G_c^B(t)G_a^B(t) \times \cos(\Delta g\beta Bt/\hbar) \quad (2)$$

$$\rho_{ss}^0(t) = \frac{1}{4} + \frac{3}{4}e^{-t/T_0}G_c^0(t)G_a^0(t) \quad (3)$$

where T_1 and T_2 are the times of spin−lattice and phase relaxation in a high field, T_0 is the parameter used to describe spin relaxation in zero field, and Δg is the difference in the *g*-factors of the radicals in the pair. The functions $G_a(t)$ and $G_c(t)$ are determined by HFC constants in the radical anion and RC, respectively, and can be calculated by methods described elsewhere.[9,18]

For a pair partner with inhomogeneous ESR line of Gaussian shape, the functions $G^0(t)$ and $G^B(t)$ in eqs 2 and 3 have the form:[18]

$$G^0(t) = \frac{1}{3}[1 + 2(1-\gamma^2\sigma^2t^2)\cdot e^{-(\gamma^2\sigma^2t^2)/2}] \quad (4)$$

$$G^B(t) = e^{-(\gamma^2\sigma^2t^2)/2} \quad (5)$$

where γ is the electron gyromagnetic ratio, and σ^2 is the second moment of the ESR spectrum for the radical anion or cation, respectively. Equations 4 and 5 were used to calculate the contributions of *p*TP radical anion and RCs with unresolved hyperfine structure.

dx.doi.org/10.1021/jp2113208 | J. Phys. Chem. A 2012, 116, 3110−3117

The available analytical solution for the $G_c(t)$ functions in the case of HFC with two groups of equivalent magnetic nuclei[19] was applied for describing the contributions of the 2,2,3-trimethylbutane and 2,2-dimethylpentane RC to the spin dynamics of the radical ion pair.

Importantly, the position of the first maximum in the TR MFE curve on the time scale can be approximated as $t \approx 1.6/(\gamma\sigma_c)$ in every case considered above. The contribution of the *p*TP radical anion to the spin dynamics is negligible due to its minor HFC constants ($\sigma_a \ll \sigma_c$) and slow paramagnetic relaxation.[20]

When the pair partner participates in chemical reactions, the description of spin evolution becomes more complicated. A single change in magnetic environment due to the reaction of the RC at time t' causes the following transformations in eqs 2 and 3:

$$\rho_{ss}^{B}(t, t') = \frac{1}{4} + \frac{1}{4}e^{-t'/T_{I1}}e^{-(t-t')/T_{II1}} + \frac{1}{2}e^{-t'/T_{I2}} \times e^{-(t-t')/T_{II2}}G_{Ic}^{B}(t')G_{IIc}^{B}(t-t')G_{a}^{B}(t) \quad (6)$$

$$\rho_{ss}^{0}(t, t') = \frac{1}{4} + \frac{3}{4}e^{-t'/T_{I0}}e^{-(t-t')/T_{II0}}G_{Ic}^{0}(t') \times G_{IIc}^{0}(t-t')G_{a}^{0}(t) \quad (7)$$

where indices "I" and "II" show that the corresponding values are determined by the parameters of either initial RC I or the product of its reaction, II. If the reaction under discussion is monomolecular or pseudomonomolecular with a rate constant k, the change of the singlet state population is described by the convolution of functions 6 and 7 with the reaction kinetics:

$$\rho_{ss}(t) = e^{-kt}\rho_{ss}(t, t) + k\int_0^t e^{-kt'}\rho_{ss}(t, t')dt' \quad (8)$$

TR MFE: Simulation Procedure. The peculiarities of the TR MFE curves assigned to the dynamic singlet−triplet transitions can be observed on the time scale of the phase relaxation time T_2, which was less than 60 ns for our systems. The TR MFE curves were simulated on this time scale to determine the HFC constants of the RCs under study. In the simulation, the optimal values of spin−lattice relaxation times T_1 were typically longer than 500 ns, and thus considerably exceed the time scale of simulation and do not significantly influence the curve shape. Thus, T_1 is derived from the fitting procedure with a low accuracy. In all cases, the experimental TR MFE curves were well fitted by theoretical ones on the assumption that the only process yielding the delayed fluorescence is the radical−ion pair recombination.

3. RESULTS AND DISCUSSION

The TR MFE curves were obtained for *n*-hexane solutions of branched alkanes, RH, listed in Table 1. No noticeable effect of the concentration of the added alkane on the shape of the fluorescence decay curves was observed. This implies that no proton transfer from $RH^{+\bullet}$ to the parent molecule takes place in our experimental conditions, because such a reaction would quench delayed fluorescence. Note that the intensities of the delayed fluorescence are comparable in similar conditions for all studied branched alkanes and are also close to those for *n*-alkanes studied earlier[12] (within a factor of 2). This indicates that the yields of solute RCs are nearly the same and makes unlikely any appreciable contribution of the proton transfer to the solvent molecule, which is expected to be different for studied RCs.

Table 1. Parameters for Modeling of the Experimental TR MFE Curves[a] as well as the Calculated Parameters of Branched Alkane RCs

radical cation	parameters for modeling of TR MFE[b]	calculated a or σ
2,2,3,3-tetramethylbutane$^{+\bullet}$[c]	1.24 (18H); g = 2.0034 $T_0 = T_2$ = 38, T_1 = 114	
2,3-dimethylbutane$^{+\bullet}$[d]	1.65 (12H), 0.64 (2H); g = 2.0034 $T_0 = T_2$ = 23, T_1 = 1000	1.56 (12H), 0.36 (2H)
2,2,4-trimethylpentane$^{+\bullet}$[d]	1.3 (10H), 0.37 (6H); g = 2.0036 $T_0 = T_2$ = 60, T_1 = 1000	1.34 (9H), 0.59 (1H) 0.25 (6H), 0.02 (2H)
2,2,3-trimethylbutane$^{+\bullet}$	1.24 (9H), 1.55 (6H); g = 2.0034 $T_0 = T_2$ = 50, T_1 = 1000	1.23 (9H), 1.48 (6H) −0.13 (1H)
2,2-dimethylpentane$^{+\bullet}$	1.33 (11H), 0.39 (3H); g = 2.0035 $T_0 = T_2$ = 30, T_1 = 1000	1.36 (9H), 0.85 (2H) 0.37 (3H), −0.15 (2H)
3,3-dimethylpentane$^{+\bullet}$	σ = 2.1; $T_0 = T_2$ = 30, T_1 = 500	σ = 2.4 (σ = 2.2[e])
2,4-dimethylpentane$^{+\bullet}$	σ = 2.0; $T_0 = T_2$ = 30, T_1 = 500	σ = 2.3 (σ = 2.0[e])
2,5-dimethylhexane$^{+\bullet}$	σ = 1.6; $T_0 = T_2$ = 13, T_1 = 500	σ = 1.7
2,2,4,4,6,8,8-heptamethylnonane$^{+\bullet}$	σ = 1.6; $T_0 = T_2$ = 20, T_1 = 500	
2,6,10,14-tetramethylpentadecane$^{+\bullet}$	σ = 0.5; g = 2.0041; $T_0 = T_2$ = 35, T_1 = 700	
squalane$^{+\bullet}$	σ = 0.4; g = 2.0039; $T_0 = T_2$ = 40, T_1 = 700	
isopropylcyclohexane$^{+\bullet}$	σ = 1.9; $T_0 = T_2$ = 15, T_1 = 500	σ = 2.1
tert-butylcyclohexane$^{+\bullet}$	σ = 2.0; $T_0 = T_2$ = 45, T_1 = 500	σ = 1.9

[a]Concentration of branched alkanes in *n*-hexane varied from 0.1 to 1 M for 2,6,10,14-tetramethylpentadecane and squalane and was equal to 0.1 M everywhere for other alkanes. a and σ in mT, relaxation times in ns. [b]In parentheses are the numbers of equivalent protons. Estimated accuracies in a and σ are 0.05 and 0.1 mT, respectively. [c]Reference 11. [d]Reference 13. [e]Taking into account fast reaction of intramolecular electron transfer (see text).

The concentration dependence of the TR MFE curves was found only for 2,6,10,14-tetramethylpentadecane and squalane solutions (see below). So, except for these two cases, the studied RCs do not participate in intermolecular electron exchange reaction, which allowed us to simulate the corresponding TR MFE curves only taking into account fast spectral exchange due to conformational transitions.

Table 1 summarizes the best fitting parameters (HFC constants or the value of σ, *g*-factors, and spin relaxation times) obtained from the TR MFE curve simulations, as well as the calculated HFC constants (or the value of σ in some cases) of RCs of the studied branched alkanes. For completeness, Table 1 also includes data for the RCs studied by us earlier.[11,13] Note, that σ-values for modeling MFE curves of 2,6,10,14-tetramethylpentadecane and squalane RC correspond to the unresolved ESR spectra in the absence of charge exchange.

The geometries and the calculated proton HFC constants of the low energy conformations for some branched alkane RCs under study are shown in Figure 1.

dx.doi.org/10.1021/jp2113208 | J. Phys. Chem. A 2012, 116, 3110−3117

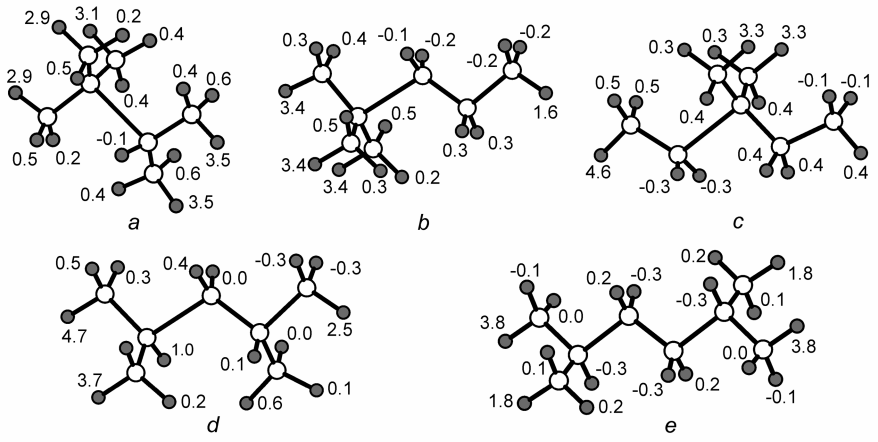

Figure 1. Geometries and HFC constants with protons (in mT) in the lowest energy conformations of 2,2,3-trimethylbutane (a), 2,2-dimethylpentane (b), 3,3-dimethylpentane (c), 2,4-dimethylpentane (d), and 2,5-dimethylhexane (e) radical cations calculated at the UB3LYP/6-31G(d) level.

To confirm the detection of the branched alkane RCs, we used the following criteria:

(1) The first was agreement of the experimental HFC constants determined by the simulation of the TR MFE curves with the results of both the low-temperature ESR studies and the quantum chemical calculations (properly averaged in every case).
(2) The second was agreement of the experimental *g*-factor with the value typical of the other branched alkane RCs.
(3) The final was charge transfer from the detected RCs to an alkane molecule with a lower ionization potential. For an olefin RC as the possible product of alkane RC decomposition, such a reaction is energetically forbidden.

Below, we consider in some detail the results of the TR MFE study and the properties of the branched alkane RCs.

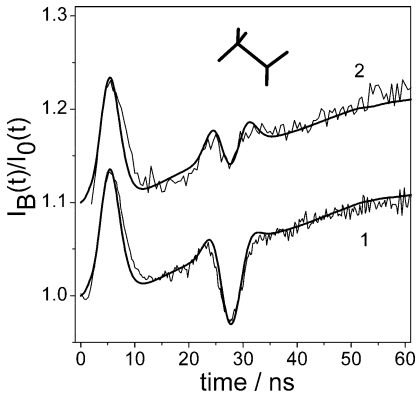

Figure 2. Experimental and calculated ratio of fluorescence intensities in high ($I_B(t)$) and zero ($I_0(t)$) magnetic fields recorded at room temperature for *n*-hexane solutions of 0.1 M 2,2,3-trimethylbutane in magnetic fields of 0.1 T (curve 1) and 1.1 T (curve 2). The concentration of *p*TP was 3×10^{-5} M in all cases. The modeling was performed using the parameters collected in Table 1.

TR MFE with Extrema Due to Equivalent Protons.

2,2,3-Trimethylbutane. Figure 2 shows that the TR MFE curves observed in the solution of this alkane clearly show two distinctive peculiarities, a peak at about 5 ns and a dip at 28 ns. The latter is more prominent at lower magnetic field (curve 1). As mentioned above, the position of the first peak is determined by the value of the second moment of the ESR spectrum of the positive charge carrier in the geminate radical ion pair. The dip on the TR MFE curve indicates that in this RC, the main contribution to HFC is made by an odd number of magnetically equivalent or nearly equivalent protons. As shown earlier,[21] its position on the time scale equals $2\pi/(\gamma a)$, where a is the characteristic HFC constant. Therefore, the TR MFE curve allows one to estimate this HFC constant as $a(H) = 1.3$ mT with an appreciable accuracy without any detailed simulation.

Evidently, the observed TR MFE curves cannot be assigned to the RC of tetramethylethylene, which is a feasible product of the 2,2,3-trimethylbutane RC cleavage, yielding the olefin RC and methane molecule. The tetramethylethylene RC has 12 equivalent protons, and for an even number of protons a distinct second peak rather than a dip would be observed in the TR MFE curve.[13]

Qualitatively, the value of the HFC constant $a(H) = 1.3$ mT is in agreement with the data obtained by the conventional ESR in low-temperature matrices. In this case, the splitting from only 5 β-protons (one proton from each methyl group) with the HFC constant $a(5H) = 3.20$ mT[22] was observed. For comparison with our result, this HFC constant should be divided by 3, because at room temperature the rotation about the C−C bonds leads to the averaging of HFC constants over the protons of methyl groups.

A more detailed analysis can be performed using the results of the quantum chemical calculations. They indicated that the unpaired electron is localized mainly at the C_2-C_3 bond of the RC. The protons of the *tert*-butyl and the two methyl groups have slightly different HFC constants (1.23 and 1.48 mT, respectively), which exceed considerably the HFC constant with the methine proton, −0.13 mT. In the simulation of the TR MFE curves, the latter was neglected, and the HFCs with two groups, consisting of 9 and 6 protons, were taken into account. The HFC constants determined by simulation (1.24 and 1.55 mT) are close to those calculated by DFT. The minor increase in the difference between the two values decreases noticeably the dip amplitude in the simulated curve with the time position remaining nearly unchanged.

The dip amplitude decreases with increasing magnetic field (Figure 2, curve 2), which is typical of the radical−ion pairs with a noticeable difference between the partner *g*-factors. This

dx.doi.org/10.1021/jp2113208 | J. Phys. Chem. A 2012, 116, 3110−3117

effect was used to determine the Δg value for the 2,2,3-trimethylbutane RC and the *p*TP radical anion. The obtained *g*-value (2.0034) of the RC is close to that of the previously studied RCs of the branched alkanes (Table 1). This is an additional evidence that the detected RC is the RC of a branched alkane.

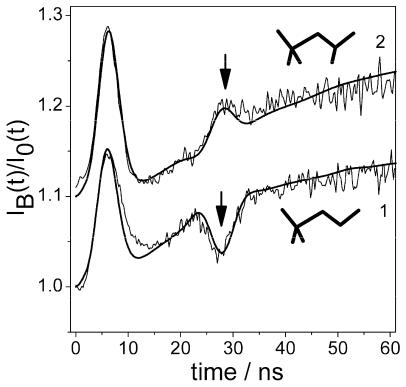

Figure 3. Experimental and calculated ratio of fluorescence intensities in high ($I_B(t)$) and zero ($I_0(t)$) magnetic fields recorded for *n*-hexane solutions of 0.1 M 2,2-dimethylpentane (curve 1) and 0.1 M 2,2,4-trimethylpentane (curve 2) in magnetic fields of 0.1 T. The concentration of *p*TP was 3×10^{-5} M in all cases. The modeling was performed using the parameters collected in Table 1. Arrows point to the peculiarities whose form (dip or peak) depends on the parity of the number of protons with the major HFC constant (see text).

2,2-Dimethylpentane. The TR MFE curve recorded for this alkane (Figure 3, curve 1) is similar to that for the 2,2,3-trimethylbutane (Figure 2). However, it has a less pronounced dip. As noted above, its position on the time scale (25−30 ns) corresponds to the main contribution of the HFC with an odd number of protons with the HFC constant $a(H) \approx 1.3$ mT.

The 2,2-dimethylpentane RC has never been observed in low-temperature matrices. The quantum chemical calculations demonstrate that in the lowest energy conformation of the 2,2-dimethylpentane RC (Figure 1b), the unpaired electron is localized mainly at the C_2-C_3 bond adjacent to the *tert*-butyl fragment. This localization is also conserved for all other conformations. Thus, the picture of spin density distribution typical of branched alkanes according to the low-temperature ESR studies[22,23] holds also for the 2,2-dimethylpentane RC.

The calculations predict that for 2,2-dimethylpentane RC two methylene β-protons (C_4 position) and nine protons of the *tert*-butyl group have large but noticeably different HFC constants at room temperature. In the simulation of the TR MFE curves, the difference was neglected, and the HFCs with two groups, consisting of 11 equivalent β-protons and 3 γ-protons, were taken into account. The position of the dip is determined by the HFC with the first group of protons (with the larger HFC constant, 1.33 mT). The small HFC constant with γ-protons (0.39 mT) decreases the dip amplitude. Note that a decrease in the amplitude may be also caused by the difference in the HFC constants of the methylene β-protons and those of the *tert*-butyl group. Table 1 demonstrates that the HFC constants obtained by simulation are close to those calculated for the protons of the *tert*-butyl fragment. The value of *g*-factor (2.0035), determined from the analysis of the TR MFE curves for different magnetic fields, is typical of the branched alkanes RC.

Note that the results for the 2,2-dimethylpentane are in qualitative agreement with those of the previously studied 2,2,4-trimethylpentane[13] that are compared in Figure 3. Both the dip at the TR MFE curves for 2,2-dimethylpentane and the weak second peak in the case of 2,2,4-trimethylpentane (indicated by arrows in Figure 3) are in agreement with the number of β-protons in the RCs of these alkanes. In both cases, the unpaired electron is localized mainly at the C_2-C_3 bond. In the case of the 2,2-dimethylbutane RC, the main contribution to HFC is made by 11 β-protons. As the 2,2,4-trimethylpentane RC has the even number of β-protons (10), the TR MFE curve exhibits the second peak rather than the dip.

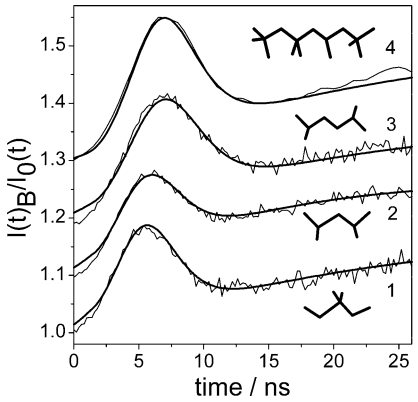

Figure 4. Experimental and calculated ratio of fluorescence intensities in high ($I_B(t)$) and zero ($I_0(t)$) magnetic fields recorded for *n*-hexane solutions of 0.1 M 3,3-dimethylpentane (curve 1), 2,4-dimethylpentane (curve 2), 2,5-dimethylhexane (curve 3), and 2,2,4,4,6,8,8-heptamethylnonane (curve 4) in magnetic fields of 0.1 T. The concentration of *p*TP was 3×10^{-5} M in all cases. The modeling was performed using the parameters collected in Table 1.

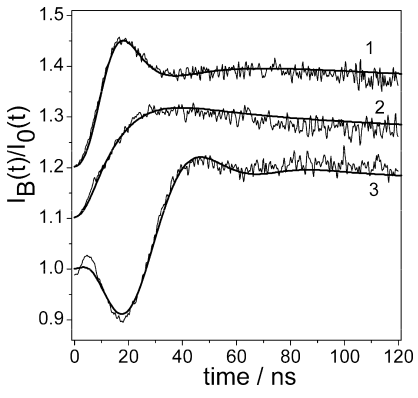

Figure 5. Experimental and calculated ratio of fluorescence intensities in high ($I_B(t)$) and zero ($I_0(t)$) magnetic fields recorded for *n*-hexane solutions of 2,6,10,14-tetramethylpentadecane: 0.1 M, $B = 0.1$ T (curve 1); 1 M, $B = 0.1$ T (curve 2); and 1 M, $B = 1$ T (curve 3). The concentration of *p*TP was 3×10^{-5} M in all cases. The modeling was performed using the parameters collected in Table 1 and the rate constant of electron exchange 3.5×10^8 M^{-1} s^{-1}.

Other Branched Acyclic Alkanes. For other branched alkanes under study, the experimental TR MFE curves have only one peak as demonstrated in Figures 4 and 5. In the

dx.doi.org/10.1021/jp2113208 | J. Phys. Chem. A 2012, 116, 3110−3117

simulation, it is the second moment of the ESR spectrum of the radical cation that can be determined with an appreciable accuracy.

3,3-Dimethylpentane. The quantum chemical calculations performed for the 3,3-dimethylpentane RC indicate that at all conformations the spin density is localized mainly at the C_2-C_3 (or C_3-C_4) bond, and this bond is elongated. Figure 1c displays the HFC constants for the lowest energy conformation showing that the spin distribution is asymmetrical. Experimentally, such asymmetry has been detected for the 3,3-dimethypentane RC in low-temperature C_8F_{18} matrices by ESR spectroscopy.[23] In that work, it was also shown that in the *n*-pentane and 3-methylpentane RCs, the spin density is also localized at the C_2-C_3 (or C_3-C_4) bond, and the unpaired electron may jump between these bonds simultaneously with the changes in their lengths. However, for the 3,3-dimethylpentane RC, this transfer was not observed in the entire experimental temperature range (up to 100 K).

On the contrary to the low-temperature matrices, in solutions at room temperature such transfer is likely to occur. Similar to the internal rotation, this transition leads to averaging of the HFC constants. This effect was taken into account in the calculations of the HFC constants in the fast exchange approximation. Such averaging of the HFC constants leads to a small decrease from 2.4 to 2.2 mT in the value of the second moment of the ESR spectrum (Table 1). Note that the value of the second moment estimated using this averaging is in better agreement with simulation, σ_c = 2.1 mT.

2,4-Dimethylpentane. As in the previous case, there are two equivalent lowest energy conformations with elongated C_2-C_3 or C_3-C_4 bonds. One of these conformations is displayed in Figure 1d. In these conformations, as in all others, the unpaired electron is localized mainly at the elongated bond. According to the calculations, the barrier of the transformation between two equivalent conformations accompanied by the spin density transfer is very low (~1.2 kcal/mol). Thus, at room temperature, the spin density transfer is very fast and causes averaging of the HFC constants. Similar to the case of the 3,3-dimethylpentane RC, this averaging gives the value σ_c = 2.0 mT of the second moment of the ESR spectrum, which is in perfect agreement with the experiment (Table 1).

2,5-Dimethylhexane. The peak at the TR MFE curve for this alkane (Figure 4, curve 3) is noticeably shifted to longer times as compared to the curves for the dimethyl-substituted pentanes (Figure 4, curves 1, 2). This corresponds to the smaller second moment of its ESR spectrum (σ = 1.6 mT) and is in agreement with the calculations (σ = 1.7 mT). In contrast to substituted pentane RCs, in the 2,5-dimethylhexane RC, the unpaired electron is not predominantly localized at one particular bond. In the lowest energy conformation (Figure 1e), the unpaired electron is delocalized over two bonds, C_2-C_3 and C_4-C_5. The same delocalization holds for the conformations obtained through rotation by 120° about these bonds. In the conformations obtained by additional 120° rotation about the C_3-C_4 bond, the spin density is localized mainly at this bond. The energies of these conformations are, however, significantly higher than that of the lowest energy one (by more than 7 kcal/mol). Thus, the population of these states at room temperature is negligible, and these conformations do not contribute to the averaged HFC constants.

2-Methylpentane and 3-Methylpentane. The TR MFE curves (not shown in figures) for these alkanes have first peaks corresponding to $\sigma \approx$ 2.1 mT and $\sigma \approx$ 1.9 mT, respectively. These values are reasonable to support the assignment of the curves features to the RCs of added methylpentanes. Note that methylpentanes are the main impurities in the used solvent, *n*-hexane. To avoid their interference, we used much higher (about 1 M) concentration of the added methylpentane as compared to that of impurity.

2,2,4,4,6,8,8-Heptamethylnonane. The value of the second moment of the ESR spectrum obtained by simulating the TR MFE curve equals 1.6 mT. No quantum chemical calculations were performed for this RC, because the number of atoms and conformations involved are very large. Note that if the spin density in this RC were localized similarly to 2,4-dimethylpentane over bonds C_2-C_4, we would obtain σ > 2 mT due to extra HFCs with the protons of two additional methyl groups at C_2 and C_4 positions. Thus, the smaller experimental value of $\sigma \approx$ 1.6 mT indicates that in this RC the spin density is delocalized through a larger number of C−C bonds.

2,6,10,14-Tetramethylpentadecane and Squalane. Experimental results for these RCs are similar to each other but differ substantially from those discussed above. The peculiarities are illustrated in Figure 5 by an example of 2,6,10,14-tetramethylpentadecane. First, the peak on the TR MFE curves is noticeably shifted to longer times. This corresponds to a decrease in the second moment of the ESR spectrum and indicates the essential delocalization of the unpaired electron. In the present work, we cannot distinguish between the delocalization due to extended molecular orbital occupied by the electron and that caused by fast intramolecular jumping between more or less localized positions.

Second, an increase in alkane concentration leads to additional shift of the observed peak to longer times that indicates the charge exchange narrowing in ESR spectrum like that for *n*-alkane RCs.[12] The TR MFE curves were simulated taking into account the spectral exchange within Gaussian-like unresolved spectrum of isolated RC by the method described earlier.[18] For both RCs, the simulation gives a similar value, $(3.5 \pm 0.5) \times 10^8$ M^{-1} s^{-1}, of the rate constant for ion-molecular charge exchange. This value is by about 2 orders of magnitude lower than the rate constant for diffusion-controlled reactions in *n*-hexane, like the electron exchange involving RCs of normal alkanes.[12] By analogy, we may suppose that for these two branched alkanes with comparatively long carbon skeleton, the electron exchange rate is, in part, diminished due to the necessity for RC to encounter an isomer of the neutral molecule with suitable geometry.

The *g*-factors of these RCs were determined in concentrated solutions of the branched alkanes to provide the spectral narrowing, which makes the effect of increasing magnetic field on the TR MFE curves more evident.

Cyclic Alkanes. The time of spin−lattice relaxation of cyclohexane RC is very short,[24] thus precluding the evaluation of its HFC constants or second moment of the ESR spectrum by TR MFE. Fortunately, the value of T_1 is longer for substituted cyclohexanes.[25] We were able to observe the first peak at the TR MFE curve and to determine the second moments of the ESR spectra for radical cations generated in solutions of *tert*-butylcyclohexane and isopropylcyclohexane. The analysis similar to that performed for branched alkanes demonstrated a fair agreement between TR MFE experiments and the quantum chemical calculations (Table 1).

Reactions between the Studied RCs and Other Alkanes. To rule out olefin RCs and to additionally support the assignment of the experimental curves to the branched

dx.doi.org/10.1021/jp2113208 | J. Phys. Chem. A 2012, 116, 3110−3117

alkane RCs, the reaction of charge transfer from the observed RCs to other alkanes was studied.

$$RH^{+\bullet} + R_1H \rightarrow RH + R_1H^{+\bullet}$$

The 1,3-dimethyladamantane (DMA) and *trans*-decalin (*t*-DEC) were chosen as electron donors, R_1H. The gas-phase ionization potentials (IPs) of these molecules (9.15 and 9.3 eV, respectively[26]) are lower than those of the branched alkanes under study. The available data[26] suggest that IPs of heptane or octane isomers are higher than or equal to 9.8 eV. For example, IP of 2,2,4-trimethylpentane is 9.89 eV. On the other hand, the IPs of DMA and *t*-DEC are higher than the IPs of olefins, which can be considered as probable products of the branched alkane RC decay. For example, RC of 2-methyl-2-pentene is a feasible product of a methane molecule detachment from a 2,2-dimethylpentane RC. The gas-phase IP of this olefin is 8.6 eV.[26] By pulse radiolysis of alkane solutions, it was shown[6] that the reaction of electron transfer is controlled by diffusion if gas-phase IP of the electron acceptor molecule exceeds that of the electron donor by 0.2 eV or more. Thus, the chosen cycloalkane molecules can easily donate their electron to the RCs of branched alkanes, whereas no electron transfer is expected to the RC of olefins.

The second reason to choose DMA and *t*-DEC as electron donors is the fast spin–lattice relaxation of their RCs. The spin–lattice relaxation time in the radical cation, measured by TR MFE, is 9 ns for DMA and 14 ns for *t*-DEC.[25] Thus, the charge transfer can be easily recognized by the acceleration of the decay of the TR MFE upon addition of these cycloalkane molecules to the solution.

Figure 6 shows the TR MFE curves for 0.1 M solution of 2,2,4-trimethylpentane without DMA and with 1 and 3 mM of DMA in *n*-hexane. As expected, the TR MFE decreases with the addition of DMA at longer times. The TR MFE curve was simulated using formulas 6–8. It was assumed that 2,2,4-trimethylpentane RC forms immediately after X-ray pulse and then participates in charge transfer reaction with DMA molecule with the rate constant *k*. This assumption seems reasonable for the given concentrations of trimethylpentane and DMA. To model spin dynamics in the 2,2,4-trimethylpentane RC, the experimental parameters summarized in Table 1 were used. Contribution to the spin dynamics of the DMA RC was taken into account using quasi-classical equations 4,5. The value of σ for the DMA RC in solution (~1 mT) was estimated from the results of the AM1 calculations of HFC constants. Note that the accuracy of σ is not critical for the simulation because of the short spin–lattice relaxation time of DMA RC.

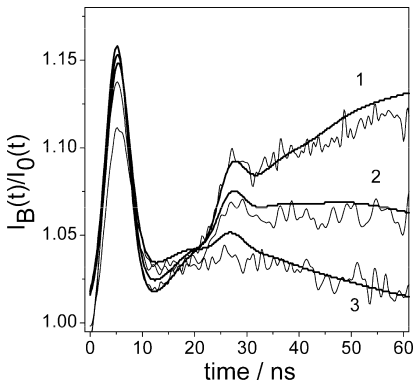

Figure 6. Experimental and calculated ratio of fluorescence intensities in high ($I_B(t)$) and zero ($I_0(t)$) magnetic fields recorded for *n*-hexane solutions of 0.1 M 2,2,4-trimethylpentane without 1,3-dimethyladamantane (curve 1), and with 1 mM (curve 2) and 3 mM (curve 3) 1,3-dimethyladamantane. In all cases, B = 0.1 T, and the concentration of *p*TP was 3×10^{-5} M.

The rate constant of the electron transfer from DMA to the 2,2,4-trimethylpentane RC was estimated from the best fit to be $k = (1.5 \pm 0.2) \times 10^{10}$ M^{-1} s^{-1}. The rate constant of the electron transfer from *t*-DEC to the 2,2,4-trimethylpentane RC was determined in a similar way and was found to be $(1.0 \pm 0.2) \times 10^{10}$ M^{-1} s^{-1}. Thus, the rate constants are close to the diffusion limit. These facts further support that in our experiments with 2,2,4-trimethylpentane solutions, the RC of alkane rather than an olefin RC is observed.

The TR MFE upon addition of DMA and *t*-DEC was studied for solutions of all heptane and octane isomers of this study. The acceleration of the decay was observed in all cases. This verifies that positive charge carriers are aliphatic radical cations in our experiments.

Lifetimes of Radical Cations. As was already mentioned, the observation of dynamic singlet–triplet transitions due to the HFCs is a reliable method of radical ion identification. These transitions are observable at times not exceeding substantially the phase relaxation time T_2. At longer time, the manifestation of any peculiarities of spin evolution is smoothed away and cannot be revealed on the TR MFE curves. Consequently, a radical ion cannot be identified with the TR MFE method at times longer than T_2. Thus, the lower limit of the lifetimes of radical cations of branched alkanes under study can be estimated to be of the order of the phase relaxation time, which is 10–60 ns in our experiments.

4. CONCLUSION

Radical cations formed in irradiated *n*-hexane solution of branched isomers of heptane, octane, and several larger alkanes were studied by the method of time-resolved magnetic field effect (TR MFE). To get the TR MFE curves, the decay of recombination fluorescence was recorded at zero and high (up to 1.1 T) external magnetic field. The time-dependent modulation was analyzed within the conventional theory of TR MFE in recombination fluorescence of spin-correlated radical ion pairs. HFC constants or ESR spectrum width and, in some cases, *g*-factors of the positive charge carriers generated in solutions were determined by simulation of the TR MFE curves. The found HFC constants were compared to that calculated using the DFT approach and averaged over accessible conformations of the radical cations of branched alkanes under study. The agreement between the calculated and observed HFC values, as well as charge transfer reaction studied, unambiguously confirms their assignment to the radical cations of branched alkanes. The lowest limit of their lifetimes in the solution at room temperature can be estimated as several tens of nanoseconds.

AUTHOR INFORMATION

Corresponding Author

*E-mail: potashov@kinetics.nsc.ru.

Notes

The authors declare no competing financial interest.

■ ACKNOWLEDGMENTS

The Program "Leading Scientific Schools", Project NS-2272.2012.3, is gratefully acknowledged.

■ REFERENCES

(1) Todres, Z. V. *Ion-Radical Organic Chemistry: Principles and Applications*; CRC Press: Boca Raton, FL, 2009.
(2) Toriyama, K. In *Radical Ionic Systems*; Lund, A., Shiotani, M., Eds.; Kluwer Academic Publishers: Dordrecht, The Netherlands, 1991; pp 99−124.
(3) Werst, D. W.; Bakker, M. G.; Trifunac, A. D. *J. Am. Chem. Soc.* **1990**, *112*, 40−50.
(4) Anisimov, O. A.; Warman, J. M.; De Haas, M. P.; De Leng, H. *Chem. Phys. Lett.* **1987**, *137*, 365−368.
(5) Shkrob, I. A.; Sauer, M. C., Jr.; Trifunac, A. D. In *Radiation Chemistry: Present Status and Future Trends*; Jonah, C. D., Rao, B. S. M., Eds.; Elsevier: Amsterdam, The Netherlands, 2001; pp 175−221.
(6) Mehnert, R. In *Radical Ionic Systems*; Lund, A., Shiotani, M., Eds.; Kluwer Academic Publishers: Dordrecht, The Netherlands, 1991; pp 231−284.
(7) Tagawa, S.; Hayashi, N.; Yoshida, Y.; Washio, M.; Tabata, Y. *Radiat. Phys. Chem.* **1989**, *34*, 503−511.
(8) Molin, Yu. N.; Anisimov, O. A. *Radiat. Phys. Chem.* **1983**, *21*, 77−82.
(9) Bagryansky, V. A.; Borovkov, V. I.; Molin, Y. N. *Russ. Chem. Rev.* **2007**, *76*, 493−506.
(10) Stass, D. V.; Anishchik, S. V.; Verkhovlyuk, V. N. In *Selectivity, Control, and Fine Tuning in High-Energy Chemistry*; Stass, D. V., Feldman, V. I., Eds.; Research Signpost: Kerala, India, 2011; pp 143−189.
(11) Bagryansky, V. A.; Borovkov, V. I.; Molin, Yu. N. *Phys. Chem. Chem. Phys.* **2004**, *6*, 924−928.
(12) Borovkov, V. I.; Gritsan, N. P.; Yeletskikh, I. V.; Bagryansky, V. A.; Molin, Y. N. *J. Phys. Chem. A* **2006**, *110*, 12752−12759.
(13) Borovkov, V. I.; Potashov, P. A.; Shchegoleva, L. N.; Bagryansky, V. A.; Molin, Y. N. *J. Phys. Chem. A* **2007**, *111*, 5839−5844.
(14) Anishchik, S. V.; Grigoryants, V. M.; Shebolaev, I. V.; Chernousov, Yu. D.; Anisimov, O. A.; Molin, Yu. N. *Prib. Tekhn. Eksp. (Russ.)* **1989**, *4*, 74−79.
(15) (a) Becke, A. D. *J. Chem. Phys.* **1993**, *98*, 5648−5654. (b) Lee, C.; Yang, W.; Parr, R. G. *Phys. Rev. B* **1988**, *37*, 785−790.
(16) Schmidt, M. W.; Baldridge, K. K.; Boatz, J. A.; Elbert, S. T.; Gordon, M. S.; Jensen, J. H.; Koseki, S.; Matsunaga, N.; Nguyen, K. A.; Su, S.; Windus, T. L.; Dupuis, M.; Montgomery, J. A. *J. Comput. Chem.* **1993**, *14*, 1347−1363.
(17) Frisch, M. J.; Trucks, G. W.; Schlegel, H. B.; et al. *Gaussian 03*, revision B.01; Gaussian, Inc.: Pittsburg, PA, 2003.
(18) Schulten, K.; Wolynes, P. G. *J. Chem. Phys.* **1978**, *68*, 3292−3297.
(19) Bagryansky, V. A.; Ivanov, K. L.; Borovkov, V. I.; Lukzen, N. N.; Molin, Yu. N. *J. Chem. Phys.* **2005**, *122*, 224503.
(20) Berndt, A.; Jones, M. T.; Lehnig, M.; Lunazzi, L.; Placucci, G.; Stegmann, H. B.; Ulmschneider, K. B. In *Numerical Data and Functional Relationship in Science and Technology*; Fisher, H., Hellwege, K.-H., Eds.; Landolt-Bornstein New Series; Springer-Verlag: Berlin−Heidelberg−New York, 1980; Group II, Vol. 9, part d1.
(21) Bagryansky, V. A.; Usov, O. M.; Borovkov, V. I.; Kobzeva, T. V.; Molin, Yu. N. *Chem. Phys.* **2000**, *255*, 237−245.
(22) Nunome, K.; Toriyama, K.; Iwasaki, M. *J. Chem. Phys.* **1983**, *79*, 2499−2503.
(23) Toriyama, K.; Okazaki, M. *J. Phys. Chem.* **1992**, *96*, 6986−6991.
(24) Borovkov, V. I.; Molin, Yu. N. *Chem. Phys. Lett.* **2004**, *398*, 422−426.
(25) Borovkov, V. I.; Molin, Yu. N. *Phys. Chem. Chem. Phys.* **2004**, *6*, 2119−2124.
(26) Lias, S. G.; Levin, R. D.; Kafafi, S. A. Ion Energetics Data. In *NIST Chemistry WebBook, NIST Standard Reference Database Number 69*; Linstrom, P. J., Mallard, W. G., Eds.; National Institute of Standards and Technology: Gaithersburg, MD, 2011; http://webbook.nist.gov (retrieved November 7, 2011).